On the Multicell Processing Capacity of the Cellular MIMO Uplink Channel in Correlated Rayleigh Fading Environment

Symeon Chatzinotas, Muhammad Ali Imran, Reza Hoshyar

Abstract

In the context of cellular systems, it has been shown that multicell processing can eliminate inter-cell interference and provide high spectral efficiencies with respect to traditional interference-limited implementations. Moreover, it has been proved that the multiplexing sum-rate capacity gain of multicell processing systems is proportional to the number of Base Station (BS) antennas. These results have been also established for cellular systems, where BSs and User Terminals (UTs) are equipped with multiple antennas. Nevertheless, a common simplifying assumption in the literature is the uncorrelated nature of the Rayleigh fading coefficients within the BS-UT MIMO links. In this direction, this paper investigates the ergodic multicell-processing sum-rate capacity of the Gaussian MIMO Cellular Multiple-Access Channel in a correlated fading environment. More specifically, the multiple antennas of both BSs and UTs are assumed to be correlated according to the Kronecker product model. Furthermore, the current system model considers Rayleigh fading, uniformly distributed User Terminals (UTs) over a planar coverage area and power-law path loss. Based on free probabilistic arguments, the empirical eigenvalue distribution of the channel covariance matrix is derived and it is used to calculate both Optimal Joint Decoding and Minimum Mean Square Error (MMSE) Filtering capacity. In addition, numerical results are presented, where the per-cell sum-rate capacity is evaluated while varying the cell density of the system, as well as the level of fading correlation. In this context, it is shown that the capacity performance is greatly compromised by BS-side correlation, whereas UT-side correlation has a negligible effect on the system's performance. Furthermore, MMSE performance is shown to be greatly suboptimal but more resilient to fading correlation in comparison to optimal decoding.

Index Terms

Information theory, Information Rates, Multiuser channels, MIMO systems, Channel correlation, Land mobile radio cellular systems, Eigenvalues and eigenfunctions.

I. Introduction

In the short history of wireless cellular systems, there has been an intense evolutionary process trying to optimize the multiple-access and coding schemes in order to provide the desired quality of service. In spite of

S. Chatzinotas, M.A. Imran and R. Hoshyar are with the Centre for Communication Systems Research, University of Surrey, United Kingdom, GU2 7XH e-mail: {S.Chatzinotas, M.Imran, R.Hoshyar}@surrey.ac.uk.

the constant improvement, one characteristic of cellular communication remained, namely its interference-limited nature. Considering the fact that the current cellular architectures are approaching their limit, the interest of both research and industry turned to cooperative techniques, such as BS cooperation, relaying and UT conferencing. In this paper, we focus on cooperating BSs which are interconnected through ideal links to a central processor, which has perfect Channel State Information (CSI). As a result, the received signals from UTs in multiple cells can be jointly processed (multicell processing). In the context of this paper, the multicell processing can be either optimal joint decoding or MMSE joint filtering, followed by single-user decoding. The capacity enhancement due to BS cooperation has been extensively studied and has been shown to grow linearly with the number of Base Station (BS) receive antennas [1], [2]. This result also applies to the case where BSs and/or UTs are equipped with multiple antennas [3], [4], [5]. However, the majority of related results have been produced based on the simplifying assumption that the fading coefficients of the MIMO subchannels are completely uncorrelated. In reality, this is not the case, since fading correlation may appear due to inadequate antenna separation and/or poor local scattering [6]. In a typical macrocellular scenario, the inadequate antenna separation mainly affects the UTs, as the components of the antenna array may be separated by a distance less than half of the communication wavelength due to their size limitations. On the other hand, poor local scattering affects mainly the BSs, as the number of local scatterers is insufficient due to their elevated position. On these grounds, this paper studies the effect of MIMO fading correlation on the capacity performance of a multicell processing system.

In this direction, it has been shown that the correlated channel matrix of the point-to-point MIMO channel can be expressed in terms of the separable variance profile, which depends on the eigenvalues of the correlation matrices. In parallel, the channel matrix of a cellular Multiple-Access (MAC) channel can be expressed in terms of the path-loss variance profile, which depends on the considered UT distribution, cell size and path loss exponent. The main objective of this study is to determine the eigenvalue distribution of the channel covariance matrix, which determines the optimal and the MMSE sum-rate capacity. For the case of point-to-point correlated MIMO channel, the objective has been accomplished by exploiting the separability of the variance profile [7], [8]. Similarly, for the case of the cellular MAC channel the asymptotic eigenvalue distribution was determined by exploiting the row-regularity of the variance profile respectively [2]. Nevertheless, the channel matrix of a correlated cellular MAC channel – expressed as Hadamard product of a separable and a row-regular variance profile – is neither separable nor row-regular and hence a new approach is needed. In this context, the main contributions of this paper can be summarized as follows:

1) A cellular MIMO uplink channel model is introduced, accommodating distributed UTs, a continuous path-loss model and Kronecker-correlated antennas.
2) Based on a recent Random Matrix Theory result, the sum-rate capacity calculation problem is transformed to a non-linear programming problem, which can be utilized to efficiently calculate the optimal capacity for finite cellular systems.
3) Furthermore, the asymptotic eigenvalue distribution of this channel model is analyzed based on free-probabilistic

arguments and closed-forms are derived for the per-cell sum-rate capacity of the optimal joint decoder and the $MMSE$ decoder.

4) Based on the derived closed-forms, it is shown that antenna correlation at the UT-side has no effect on the performance, while antenna correlation at the BS-side compromises the multiplexing gain of the system.
5) For a set of practical parameters, the agreement of analytical closed-forms and Monte Carlo simulations is established and the effect of BS-side antenna correlation is evaluated.

The remainder of this paper is structured as follows: Section II provides a detailed review of the MIMO correlation and multicell processing uplink channel models. Section III defines the considered channel model and describes the derivation of the optimal and MMSE capacity closed-forms. Section V verifies the accuracy of the analysis by comparing with Monte Carlo simulations and presents the practical results obtained for a typical macrocellular scenario. Section VI concludes the paper.

A. Notation

Throughout the formulations of this paper, R is the cell radius, N is the number of BSs, K is the number of UTs per cell and η is the power-law path loss exponent. Additionally, n_{BS} and n_{UT} are the number of multiple antennas at each Base Station (BS) and each User Terminal (UT) respectively. $\mathbb{E}[\cdot]$ denotes the expectation, $(\cdot)^*$ denotes the complex conjugate, $(\cdot)^\dagger$ denotes the conjugate transpose matrix, $\odot$ denotes the Hadamard product, $\otimes$ denotes the Kronecker product and $\asymp$ denotes asymptotic equivalence of the eigenvalue distributions. The norm of a complex scalar is denoted by $|\cdot|$, whereas the Frobenius norm of a matrix or vector is denoted by $\|\cdot\|$. The inequality $\mathbf{A} \succeq \mathbf{B}$, where $\mathbf{A}, \mathbf{B}$ are positive semidefinite matrices, denotes that $\mathbf{A} - \mathbf{B}$ is also positive semidefinite.

II. Related Work & Preliminaries

A. Correlated MIMO Channel Models

Focusing on a point-to-point MIMO link, the channel matrix can be expressed in general as [9]:

$$\mathbf{H} = \mathbf{R}_R^{1/2} \mathbf{G}_R \mathbf{R}_H^{1/2} \mathbf{G}_T \mathbf{R}_T^{1/2}, \tag{1}$$

where $\mathbf{G}_R$ and $\mathbf{G}_T$ are Gaussian matrices, whereas $\mathbf{R}_R$, $\mathbf{R}_H$ and $\mathbf{R}_T$ are deterministic or slow-varying matrices. The matrices $\mathbf{R}_R$ and $\mathbf{R}_T$, also known as the receive and transmit correlation matrix, depend on the angle spread, the antenna beamwidth and the antenna spacing at the receive and the transmit end respectively. The matrix $\mathbf{R}_H$ introduces the notion of the keyhole or pinhole channel, which appears when $\mathbf{R}_H$ is a low-rank matrix. In cases where there is adequate scattering to prevent the keyhole effects (i.e. $\mathbf{R}_H$ is full-rank), the channel matrix can be written as:

$$\mathbf{H} = \mathbf{R}_R^{1/2} \mathbf{G} \mathbf{R}_T^{1/2}, \tag{2}$$

where $\mathbf{G}$ is a Gaussian matrix. This channel matrix represents the *Kronecker correlation model* [10], since the covariance of the vectorized channel matrix can be written as the Kronecker product of the receive and transmit

correlation matrix, namely:

$$\mathrm{cov}\left(\mathrm{vec}\left(\mathbf{H}\right)\right) = \mathbf{R}_R \otimes \mathbf{R}_T \tag{3}$$

or equivalently

$$\mathbb{E}\left[\left(\mathbf{H}\right)_{pq}\left(\mathbf{H}\right)^*_{rs}\right] = \left(\mathbf{R}_R\right)_{pr}\left(\mathbf{R}_T\right)_{qs}, \tag{4}$$

where $\left(\mathbf{X}\right)_{ij}$ is the (i,j)th element of matrix $\mathbf{X}$. According to the Kronecker correlation model, the correlation between two subchannels equals to the product of the corresponding transmit and receive correlation (c.f. Equation (4)). From a physical point-of-view, the Kronecker model appears when the antennas are arranged in regular arrays and the correlation vanishes fast with distance [7]. In this point, it is worth mentioning that according to [11], [12] a MIMO channel with a large number of keyholes converges to the Kronecker MIMO model. An interesting property of the Kronecker model is its equivalency to the *separable correlation model* [7], [8] , while studying the eigenvalue distribution of the channel covariance matrix $\mathbf{H}\mathbf{H}^\dagger$. More specifically, if $\mathbf{R}_R = \mathbf{U}\mathbf{D}_R\mathbf{U}^\dagger$ and $\mathbf{R}_T = \mathbf{V}\mathbf{D}_T\mathbf{V}^\dagger$ are the eigenvalue decompositions of the receive and transmit correlation matrices respectively, then -based on the isotropic behavior of Gaussian matrices- the eigenvalue distribution of $\mathbf{H}\mathbf{H}^\dagger = \mathbf{R}_R^{1/2}\mathbf{G}\mathbf{R}_T\mathbf{G}^\dagger\mathbf{R}_R^{1/2}$ is equivalent to the one of $\mathbf{D}_R^{1/2}\mathbf{G}\mathbf{D}_T\mathbf{G}^\dagger\mathbf{D}_R^{1/2}$. In this direction, the equivalent MIMO channel matrix can be written as:

$$\mathbf{H} \asymp \mathbf{D}_R^{1/2}\mathbf{G}\mathbf{D}_T^{1/2}. \tag{5}$$

This equivalency is going to be very useful in the derivations of Section III.

Let us now focus on the structure of the correlation matrix. A common model often used to effectively quantify the level of spatial correlation is the exponential correlation model [13], [14], [15] . More specifically, according to the exponential model,the receive/transmit correlation matrix can be constructed utilizing a single coefficient $\rho_e \in \mathbb{C}$ with $|\rho_e| \leq 1$ as follows:

$$R_{ij} = \begin{cases} \left(\rho_e\right)^{\mathrm{abs}(j-i)}, & i \leq j \\ \left(\left(\rho_e\right)^{\mathrm{abs}(j-i)}\right)^*, & i > j \end{cases} \tag{6}$$

where $\mathrm{abs}(\cdot)$ denotes the absolute value. It has been shown that the exponential model can approximate the correlation in a uniform linear array under rich scattering conditions [16]. Similar correlation models, such as the square exponential and the tridiagonal model can be found in [17].

B. Point-to-point MIMO channel capacity

The already existing approaches for the point-to-point MIMO channel can be classified in two main categories: exact analysis and asymptotic analysis. In the exact analysis, the probability distributions of finite-dimension matrices are investigated, resulting in closed forms which can produce exact results. On the other hand, in the asymptotic analysis a single or both dimensions of the random channel matrix grow infinitely large in order to allow approximations and simplifications due to the law of large numbers. Although the asymptotic analysis may seem less accurate, it has been widely shown that asymptotic closed forms are able to produce accurate results even for finite dimensions [18]. What is more, the asymptotic analysis is ideal for studying cases where the system size

is of no importance, since it reveals the effect of normalized parameters and provides insights into the system's performance [19]. In the category of asymptotic analysis, the majority of the approaches consider the generic setting where correlation affects both transmit and receive end and the numbers of both transmit and receive antennas grow large together while preserving a fixed ratio. Although the asymptotic eigenvalue distribution analysis comprises an approximation for matrices of finite dimensions, it is often employed in order to isolate the effect of specific physical parameters and to produce analytical closed forms. This setting is particularly suitable for studying the uplink channel of multicell processing cellular systems, since the ratio of transmit and receive antennas is a constant proportional to the per-cell number of UTs K.

The performance of multi-antenna channels was originally investigated in [20], [21] and it was shown that the capacity grows linearly with $\min(n_r, n_t)$, where n_r and n_t are the number of receive and transmit antennas respectively. However, the correlated fading amongst the multiple antennas compromises the capacity performance with respect to the independent fading case. This phenomenon is widely established in various regimes and settings; the capacity of the Kronecker correlated (a.k.a. doubly correlated) MIMO channel is expressed as a fixed-point equation based on the Steltjes' transform [7] of the limiting eigenvalue distribution of $\mathbf{HH}^{\dagger}$. In the same direction, authors in [22] study the capacity of the Kronecker correlated MIMO channel based on the principles of Random Matrix Theory [18]. The derivation results in a fixed-point equation including functionals of the $SINR$ and $MMSE$. In [23] and [8], the expectation and the variance of the capacity are evaluated using closed forms based on the solution of 2×2 equation systems. In [24], the principles of majorization theory [25] are applied in order to show that the average mutual information is a Schur-concave function with respect to the ordered eigenvalue vector of the correlation matrix. In addition, the doubly correlated MIMO channel for Toeplitz correlation matrices is analyzed in [17] based on the concept of linear spectral statistics. Finally, in [26], [27] the performance of Kronecker correlated MIMO channels is studied using the replica method, which originates in theoretical physics.

It should be noted that the aforementioned results specifically focus on the point-to-point correlated MIMO channel. In the following paragraph, we describe the channel characteristics of a multiple-access channel which is the information-theoretic basis of the cellular uplink channel.

C. Cellular uplink models

This section focuses on the evolution of channel modelling in the area of BS cooperation. The description starts with single-antenna cellular systems and concludes with the extension of the channel model for multiple-antennas at both transmit and receive ends. The Gaussian Cellular Multiple-Access Channel (GCMAC) has been the starting point for studying the Shannon-theoretic limits of cellular systems. It all began with Wyner's model [28], which assumes that all the UTs in the cell of interest have equal channel gains, which are normalized to 1. It considers interference only from the UTs of the two neighboring cells, which are all assumed to have a fixed channel gain, also known as interference factor α, which ranges in $[0, 1]$. Assuming that there is a power-law path loss model which affects the channel gain, Wyner has modeled the case where the UTs of each cell are collocated with the cell's BS, since no distance-dependent degradation of the channel gain is considered. The same assumption is made

by Somekh-Shamai [1], which have extended Wyner's model for flat fading environment. In both [28] and [1], a single interference factor α is utilized to model both the cell density and the path loss. The interference factor α ranges in $[0,1]$, where $\alpha=0$ represents the case of perfect isolation among the cells and $\alpha=1$ represents the case of BSs' collocation, namely a MIMO MAC channel. Subsequently, the models in [29], [4] were presented, which differ from the aforementioned models in the sense that they consider interference from all the cells of the system (i.e. multiple-tier interference). In [4], the multiple-tier interference model is combined with multiple antennas and the asymptotic performance of optimal and group $MMSE$ decoders is derived for orthogonal intra-cell UTs. In [29], an interference coefficient is defined for each BS-UT link based on the power-law path loss model. Although the author in [29] takes into account a more realistic structure of the path loss effect, the UTs of each cell have still equal channel gain and this refers to the case where the UTs of each cell are collocated with the cell's BS. Nevertheless, this model is more detailed than the previously described models, since it decomposes the interference factor α, so that the cell density/radius and the path loss exponent can be modelled and studied separately. Finally, the model used in [30] extends the previous models by considering that the UTs are no longer collocated, but they can be (uniformly) distributed across the cell's coverage area. In this point, it should be noted that for all the aforementioned Gaussian multiple-access channel models the optimal capacity-achieving transmission strategy is superposition coding over the available bandwidth [31], [1]. In other words, the ensemble of system UTs transmits simultaneously over the same bandwidth.

In the latter model [30], by assuming power-law path loss, flat fading and uniformly distributed UTs, the received signal at cell n, at time index i, is given by:

$$y^n[i]=\sum_{m=1}^{N}\sum_{k=1}^{K}\varsigma_k^{nm}g_k^{nm}[i]x_k^m[i]+z^n[i], \tag{7}$$

where $x_k^m[i]$ is the ith complex channel symbol transmitted by the kth UT of the mth cell and $\{g_k^{nm}\}$ are independent, strictly stationary and ergodic complex random processes in the time index i, which represent the flat fading processes experienced in the transmission path between the nth BS and the kth UT in the mth cell. The fading coefficients are assumed to have unit power, i.e. $\mathbb{E}[|g_k^{nm}[i]|^2]=1$ for all (n,m,k) and all UTs are subject to an average power constraint, i.e. $\mathbb{E}[|x_k^m[i]|^2]\leq P$ for all (m,k). The interference factors ς_k^{nm} in the transmission path between the mth BS and the kth UT in the nth cell are calculated according to the "modified" power-law path loss model [29], [32]:

$$\varsigma_k^{nm}=\left(1+d_k^{nm}\right)^{-\eta/2}. \tag{8}$$

Dropping the time index i, the aforementioned model can be more compactly expressed as a vector memoryless channel of the form:

$$\mathbf{y}=\mathbf{H}\mathbf{x}+\mathbf{z}. \tag{9}$$

The channel matrix $\mathbf{H}$ can be written as,

$$\mathbf{H}=\mathbf{\Sigma}\ \odot\ \mathbf{G}, \tag{10}$$

where $\mathbf{\Sigma}$ is a $N \times KN$ deterministic matrix and $\mathbf{G}$ is a Gaussian $N \times KN$ matrix with complex circularly symmetric (c.c.s.) independent identically distributed (i.i.d.) elements of unit variance, comprising the corresponding Rayleigh fading coefficients. The entries of the $\mathbf{\Sigma}$ matrix are defined by the variance profile function

$$\varsigma\Big(u, v\Big) = \Big(1 + d\,(u, v)\Big)^{-\eta/2}, \tag{11}$$

where $u \in [0, 1]$ and $v \in [0, K]$ are the normalized indices for the BSs and the UTs respectively and $d\,(u, v)$ is the normalized distance between BS u and user v. In the case of multiple UT and/or BS antennas (n_{UT} and n_{BS} respectively), the channel matrix $\mathbf{H}$ can be written as,

$$\mathbf{H} = \mathbf{\Sigma}_M \ \odot \mathbf{G}_M, \tag{12}$$

where $\mathbf{G}_M$ is a standard complex Gaussian $Nn_{BS} \times KNn_{UT}$ matrix with elements of unit variance, comprising the Rayleigh fading coefficients between the KNn_{UT} transmit and the Nn_{BS} receive antennas. Similarly, $\mathbf{\Sigma}_M$ is a $Nn_{BS} \times KNn_{UT}$ deterministic matrix, comprising the path loss coefficients between the KNn_{UT} transmit and the Nn_{BS} receive antennas. Since the multiple antennas of each UT / BS are collocated, $\mathbf{\Sigma}_M$ can be written as a block matrix based on the variance profile matrix $\mathbf{\Sigma}$ of Equation (10)

$$\mathbf{\Sigma}_M = \mathbf{\Sigma} \otimes \mathbf{J}, \tag{13}$$

where $\mathbf{J}$ is a $n_{BS} \times n_{UT}$ matrix of ones.

III. Channel Model & Assumptions

Let us assume that K UTs are uniformly distributed in each cell of a planar cellular system (Fig. 1) comprising N base stations and that each BS and each UT are equipped with n_{BS} and n_{UT} antennas respectively. Under conditions of correlated flat fading, the received signal at cell n, at time index i, is given by:

$$\mathbf{y}^n[i] = \sum_{m=1}^{N} \sum_{k=1}^{K} \varsigma_k^{nm}\, (\mathbf{R}_{\mathbf{R}_k}^{nm})^{\frac{1}{2}}\, \mathbf{G}_k^{nm}[i]\, (\mathbf{R}_{\mathbf{T}_k}^{nm})^{\frac{1}{2}}\, \mathbf{x}_k^m[i] + \mathbf{z}^n[i], \tag{14}$$

where $\mathbf{x}_k^m[i]$ is the ith complex channel symbol vector $n_{UT} \times 1$ transmitted by the kth UT of the mth cell and $\{\mathbf{G}_k^{nm}\}$ is a $n_{BS} \times n_{UT}$ random matrix with independent, strictly stationary and ergodic complex random elements in the time index i. According to the Kronecker correlation model, $\mathbf{R}_{\mathbf{T}_k}^{nm}$ and $\mathbf{R}_{\mathbf{R}_k}^{nm}$ are deterministic transmit and receive correlation matrices of dimensions $n_{UT} \times n_{UT}$ and $n_{BS} \times n_{BS}$ respectively. In this context, the following normalizations are considered in order to ensure that the correlation matrices do not affect the path loss gain of the BS-UT links: $\mathrm{tr}\,(\mathbf{R}_{\mathbf{T}_k}^{nm}) = n_{UT}$ and $\mathrm{tr}\,(\mathbf{R}_{\mathbf{R}_k}^{nm}) = n_{BS}$ for all (n, m, k). The matrix product $(\mathbf{R}_{\mathbf{R}_k}^{nm})^{\frac{1}{2}}\, \mathbf{G}_k^{nm}[i]\, (\mathbf{R}_{\mathbf{T}_k}^{nm})^{\frac{1}{2}}$ represents the multiple-antenna correlated flat fading processes experienced in the transmission path between the n_{BS} receive antennas of the nth BS and the n_{UT} transmit antennas of the kth UT in the mth cell. The fading coefficients are assumed to have unit power, i.e. $\mathbb{E}_i[\mathbf{G}_k^{nm}[i]\mathbf{G}_k^{nm}[i]^\dagger] = \mathbf{I}$ for all (n, m, k) and all UTs are subject to a power constraint P, i.e. $\mathbb{E}_i[\boldsymbol{x}_k^m[i]\boldsymbol{x}_k^m[i]^\dagger] \preceq \frac{P}{n_{UT}}\mathbf{I}_{n_{UT}}$ for all (m, k). The vector $\mathbf{z}^n[i]$ represents the AWGN noise at the receiver with $\mathbb{E}[\mathbf{z}^n[i]] = \mathbf{0},\ \mathbb{E}[\mathbf{z}^n[i]\mathbf{z}^{\mathbf{n}}[i]^\dagger] = \sigma^2\mathbf{I}$. To simplify notations, the parameter $\gamma = P/\sigma^2$ is defined as the UT transmit power normalized by the receiver noise power. The variance

coefficients ς_k^{nm} in the transmission path between the mth BS and the kth UT in the nth cell are calculated according to the "modified" power-law path loss model (cf. (8)). Dropping the time index i, the aforementioned model can be more compactly expressed as a vector memoryless channel of the form

$$\mathbf{Y} = \mathbf{H}\mathbf{X} + \mathbf{Z}, \tag{15}$$

where $\mathbf{Y} = [\mathbf{y}^{(1)} ... \ \mathbf{y}^{(N)}]^T$ with $\mathbf{y}^{(n)} = [y^1 ... \ y^{n_{BS}}]$ representing the received signal vector by the n_{BS} antennas of the nth BS, $\mathbf{X} = [\mathbf{x}_{(1)}^{(1)} \dots \mathbf{x}_{(K)}^{(1)} \mathbf{x}_{(1)}^{(2)} \dots \ \dots \mathbf{x}_{(K)}^{(N-1)} \mathbf{x}_{(1)}^{(N)} \dots \mathbf{x}_{(K)}^{(N)}]^T$ with $\mathbf{x}_{(k)}^{(n)} = [x^1 ... \ x^{n_{UT}}]$ representing the transmit signal vector by the n_{UT} antennas of the kth UT in the nth cell and $\mathbf{Z}$=$[\mathbf{z}^{(1)} ... \ \mathbf{z}^{(N)}]^T$ with $\mathbf{z}^{(n)} = [z^1 ... \ z^{n_{BS}}]$ being i.i.d c.c.s. random variables representing AWGN. In order to simplify the notations, it is assumed that all BSs/UTs are characterized by identical receive $\mathbf{R_R}$ and transmit $\mathbf{R_T}$ correlation matrices. However, it should be noted that the following analysis can be straightforwardly generalized to encompass the more realistic case of different correlation matrices for each BS/UT. The channel matrix $\mathbf{H}$ can be written as

$$\mathbf{H} = \mathbf{\Sigma_M} \odot \ \left(\left(\mathbf{I}_N \otimes \mathbf{R_R}^{\frac{1}{2}} \right) \mathbf{G_M} \left(\mathbf{I}_{KN} \otimes \mathbf{R_T}^{\frac{1}{2}} \right) \right), \tag{16}$$

where $\mathbf{G_M}$ is a $Nn_{BS} \times KNn_{UT}$ Gaussian matrix with i.i.d. c.s.s. elements of unit variance. As explained before, the Kronecker correlation model is equivalent to a separable variance profile model in terms of its eigenvalue distribution. Based on this equivalence, the channel matrix can be rewritten as follows:

$$\begin{aligned} \mathbf{H} &= \mathbf{\Sigma_M} \odot \ \left(\left(\mathbf{I}_N \otimes \mathbf{R_R}^{\frac{1}{2}} \right) \mathbf{G_M} \left(\mathbf{I}_{KN} \otimes \mathbf{R_T}^{\frac{1}{2}} \right) \right) \\ &\asymp \mathbf{\Sigma_M} \odot \ \left(\tilde{\mathbf{D}}_{\mathbf{R}}^{\frac{1}{2}} \mathbf{G_M} \tilde{\mathbf{D}}_{\mathbf{T}}^{\frac{1}{2}} \right) \\ &= \mathbf{\Sigma_M} \odot \left(\tilde{\mathbf{d}}_{\mathbf{R}}^{\dagger} \tilde{\mathbf{d}}_{\mathbf{T}} \right)^{\frac{1}{2}} \odot \ \mathbf{G_M} \end{aligned} \tag{17}$$

where $\tilde{\mathbf{D}}_{\mathbf{R}}$ and $\tilde{\mathbf{D}}_{\mathbf{T}}$ are the diagonal eigenvalue matrices of $\mathbf{I}_{N\times N} \otimes \mathbf{R_R}$ and $\mathbf{I}_{N\times N} \otimes \mathbf{R_T}$ respectively and $\tilde{\mathbf{d}}_{\mathbf{R}}$ and $\tilde{\mathbf{d}}_{\mathbf{T}}$ are row vectors containing the diagonal elements of $\tilde{\mathbf{D}}_{\mathbf{R}}$ and $\tilde{\mathbf{D}}_{\mathbf{T}}$ respectively. As it can be seen, the MIMO correlation model has been transformed into an uncorrelated model with a variance profile $\mathbf{\Omega} = \mathbf{\Sigma_M} \odot (\tilde{\mathbf{d}}_{\mathbf{R}}^{\dagger} \tilde{\mathbf{d}}_{\mathbf{T}})^{\frac{1}{2}}$, which is neither row regular nor separable.

IV. Eigenvalue Distribution Analysis & Capacity Results

A. A Random Matrix Theory approach

On the basis of a recent result in Random Matrix Theory [33, Theorem 2.4 and Theorem 4.1] the optimal per-cell sum-rate capacity of the derived channel model is given by:

$$C_{\text{opt}}(\gamma, N, n_{BS}, K, n_{UT}) = \frac{1}{N} \left(\log\det\left(\frac{\gamma}{n_{UT}} \mathbf{T}^{-1} \right) + \log\det\left(\frac{\gamma}{n_{UT}} \tilde{\mathbf{T}}^{-\mathbf{1}} \right) - \frac{1}{KN\gamma} \left\| \mathbf{\Omega} \odot \left(\mathbf{t}^T \tilde{\mathbf{t}} \right)^{\frac{1}{2}} \right\|^2 \right) \tag{18}$$

where $\mathbf{T}$ and $\tilde{\mathbf{T}}$ are given as the solution of the following $Nn_{BS} + KNn_{UT}$ equations:

$$t_i = \frac{\gamma}{1 + \frac{1}{KNn_{UT}} \text{tr}\left(\tilde{\mathbf{\Omega}}_i \tilde{\mathbf{T}} \right)} \quad \text{for} \quad i = 1 \dots Nn_{BS} \tag{19}$$

$$\tilde{t}_j = \frac{\gamma}{1 + \frac{1}{KNn_{UT}} \mathrm{tr}\left(\mathbf{\Omega}_j \mathbf{T}\right)} \quad \text{for} \quad j = 1 \dots KNn_{UT} \tag{20}$$

with the unknown variables

$$\mathbf{T} = \mathrm{diag}\left(\mathbf{t}\right) \quad \text{and} \quad \mathbf{t} = [t_1 \dots t_{Nn_{BS}}]$$

$$\tilde{\mathbf{T}} = \mathrm{diag}\left(\tilde{\mathbf{t}}\right) \quad \text{and} \quad \tilde{\mathbf{t}} = [\tilde{t}_1 \dots \tilde{t}_{KNn_{UT}}]$$

and

$$\mathbf{\Omega}_j = \mathrm{diag}\left(\boldsymbol{\omega}_j\right)^2 \quad \text{where} \quad \boldsymbol{\omega}_j = [\omega_{1j} \dots \omega_{Nn_{BS}j}] \text{ is the } j\text{th column of } \mathbf{\Omega}$$

$$\tilde{\mathbf{\Omega}}_i = \mathrm{diag}\left(\boldsymbol{\omega}_i\right)^2 \quad \text{where} \quad \boldsymbol{\omega}_i = [\omega_{i1} \dots \omega_{iKNn_{UT}}] \text{ is the } i\text{th row of } \mathbf{\Omega}$$

This result simplifies the capacity computation in large systems by converting the original problem to a non-linear programming problem. Hence, this approach can be utilized to efficiently calculate the optimal capacity for finite cellular systems. However, the size of the problem i.e. the number of equations still depends on the size of the system N and thus this solution cannot provide asymptotic results.

B. A Free Probability Approach

This section describes a free probability approach which can be utilized to derive a closed form for the probability density function of the asymptotic eigenvalue distribution. Firstly, the uncorrelated model is studied, followed by the transmit and receive single-side correlation model. Subsequently, the produced results for the single-side case are utilized to deduce the solution for the double-side case. In this point, it should be noted that free probability theory was established by Voiculescu [34] and it has been also used in [14], [15] to investigate the case of point-to-point MIMO channels correlated on a single side according to the exponential model.

1) Uncorrelated Point-to-point Channel: In this case, there is no variance profile or equivalently the variance profile is matrix of ones. Therefore, considering a Gaussian channel matrix $\mathbf{G} \sim \mathcal{CN}\left(\mathbf{0}, \mathbf{I}\right)$, the empirical eigenvalue distribution of $\frac{1}{N}\mathbf{G}^\dagger\mathbf{G}$ converges almost surely (a.s.) to the non-random limiting eigenvalue distribution of the Marčenko-Pastur law [35], whose Shannon transform is given by

$$\mathcal{V}_{\frac{1}{N}\mathbf{G}^\dagger\mathbf{G}}(y) \xrightarrow{a.s.} \mathcal{V}_{\mathrm{MP}}(y,\beta) \tag{21}$$

$$\text{where} \quad \mathcal{V}_{\mathrm{MP}}\left(y,\beta\right) = \log\left(1 + y - \frac{1}{4}\phi\left(y,\beta\right)\right) + \frac{1}{\beta}\log\left(1 + y\beta - \frac{1}{4}\phi\left(y,\beta\right)\right) - \frac{1}{4\beta y}\phi\left(y,\beta\right)$$

$$\phi\left(y,\beta\right) = \left(\sqrt{y\left(1+\sqrt{\beta}\right)^2 + 1} - \sqrt{y\left(1-\sqrt{\beta}\right)^2 + 1}\right)^2$$

and η-transform is given by [36, p. 303]

$$\eta_{\mathrm{MP}}\left(y,\beta\right) = 1 - \frac{\phi\left(y,\beta\right)}{4\beta y} \tag{22}$$

where β is the ratio of the horizontal to the vertical dimension of the $\mathbf{G}$ matrix. The transforms of the Marčenko-Pastur law are going to be useful in the capacity derivations of the uncorrelated case.

2) Uncorrelated Cellular Channel: In this case, there is a row-regular path-loss variance profile and thus the channel matrix is written as $\mathbf{H} = \mathbf{\Sigma_M} \odot \mathbf{G_M}$. For the sake of completeness, we include the derivation of the asymptotic eigenvalue distribution of $\frac{1}{N}\mathbf{H}\mathbf{H}^\dagger$ based on the analysis in [29]. In this direction, $\frac{1}{N}\mathbf{H}^\dagger\mathbf{H}$ can be written as the sum of $KNn_{UT} \times KNn_{UT}$ unit rank matrices, i.e.

$$\frac{1}{N}\mathbf{H}^\dagger\mathbf{H} = \sum_{i=1}^{Nn_{BS}} \mathbf{h}_i^\dagger \mathbf{h}_i \tag{23}$$

where $\mathbf{h}_i \sim \mathcal{CN}(\mathbf{0}, \mathbf{V}_i)$ denotes the ith $1 \times KNn_{UT}$ row vector of $\frac{1}{\sqrt{N}}\mathbf{H}$, since the term $\frac{1}{N}$ has been incorporated in the unit rank matrices. The covariance matrix equals $\mathbf{V}_i = \frac{1}{N}\left(\mathrm{diag}(\boldsymbol{\sigma}_i)\right)^2$, where $\mathrm{diag}(\boldsymbol{\sigma}_i)$ stands for a diagonal matrix with the elements of vector $\boldsymbol{\sigma}_i$ across the diagonal with $\boldsymbol{\sigma}_i$ being the ith row of $\mathbf{\Sigma_M}$. The unit-rank matrices $\mathbf{W}_i = \mathbf{h}_i^\dagger \mathbf{h}_i$ constitute complex singular Wishart matrices with one degree of freedom and their density according to [37, Theorem 3-4] is

$$\begin{aligned} f_{\mathbf{V}_i}(\mathbf{W}_i) &= B_{\mathbf{V}_i}^{-1} \det\left(\mathbf{W}_i\right)^{1-Kn_{UT}N} e^{-\mathrm{tr}\left(\mathbf{V}_i^{-1}\mathbf{W}_i\right)} \\ B_{\mathbf{V}_i} &= \pi^{Kn_{UT}N-1} \det\left(\mathbf{V}_i\right). \end{aligned} \tag{24}$$

If $\mathbf{h}_i^\dagger = \mathbf{Q}_i\mathbf{S}_i$ is a singular value decomposition, then the density can be written as

$$f_{\mathbf{V}_i}(\mathbf{W}_i) = B_{\mathbf{V}_i}^{-1} \det\left(\mathbf{S}_i\mathbf{S}_i^\dagger\right)^{1-Kn_{UT}N} e^{-\mathrm{tr}\left(\mathbf{V}_i^{-1}\mathbf{Q}_i\mathbf{S}_i\mathbf{S}_i^\dagger\mathbf{Q}_i^\dagger\right)}. \tag{25}$$

It can be easily seen that if $\mathbf{V}_i = \mathbf{I}$, the matrices would be unitarily invariant [38, Definition 17.7] and therefore asymptotically free [39]. Although in our case $\mathbf{V}_i = \frac{1}{N}\left(\mathrm{diag}(\boldsymbol{\sigma}_i)\right)^2$, we assume that the asymptotic freeness still holds. Similar approximations have been already investigated in an information-theoretic context, providing useful analytical insights and accurate numerical results [40], [41]. In this context, the R-transform of each unit rank matrix [18, Example 2.28] is given by

$$\mathcal{R}_{\mathbf{h_i}^\dagger\mathbf{h_i}}(w) = \frac{1}{Kn_{UT}N} \frac{\|\mathbf{h}_i\|^2}{1 - w\|\mathbf{h}_i\|^2} \tag{26}$$

and the asymptotic R-transform of $\mathbf{H}^\dagger\mathbf{H}$ is equal to the sum of the R-transforms of all the unit rank matrices [18, Theorem 2.64]

$$\begin{aligned} \lim_{N\to\infty} \mathcal{R}_{\frac{1}{N}\mathbf{H}^\dagger\mathbf{H}}(w) &\simeq \lim_{N\to\infty} \sum_{i=1}^{Nn_{BS}} \mathcal{R}_{\mathbf{h_i}^\dagger\mathbf{h_i}}(w) \\ &= \lim_{N\to\infty} \frac{1}{Kn_{UT}N} \sum_{i=1}^{Nn_{BS}} \frac{\|\mathbf{h}_i\|^2}{1 - w\|\mathbf{h}_i\|^2} \end{aligned} \tag{27}$$

Since the variance profile function of Equation (11) defines rectangular block-circulant matrix with $1 \times K$ blocks which is symmetric about $u = Kv$, the channel matrix $\mathbf{H}$ is asymptotically row-regular [18, Definition 2.10] and thus the asymptotic norm of $\mathbf{h}_i$ converges to a deterministic constant for every BS, i.e $\forall i$

$$\lim_{N\to\infty} \|\mathbf{h}_i\|^2 = \lim_{N\to\infty} \frac{1}{N} \sum_{j=1}^{KNn_{UT}} \varsigma_{ij}^2 = \int_0^{Kn_{UT}} \varsigma^2(u,v)dv \tag{28}$$

where ς_{ij} is the (i,j)th element of the $\mathbf{\Sigma_M}$ matrix. In addition, based on the row-regularity it can be seen that $\forall v$

$$n_{BS}\int_0^{Kn_{UT}}\varsigma^2(u,v)dv=\int_0^{n_{BS}}\int_0^{Kn_{UT}}\varsigma^2(u,v)dudv. \tag{29}$$

Therefore, Equation (27) can be simplified to [18, Theorem 2.31, Example 2.26]

$$\begin{aligned}\lim_{N\to\infty}\mathcal{R}_{\frac{1}{N}\mathbf{H}^\dagger\mathbf{H}}(w)&\simeq\frac{1}{Kn_{UT}}\int_0^{n_{BS}}\frac{\int_0^{Kn_{UT}}\varsigma^2(u,v)dv}{1-w\int_0^{Kn_{UT}}\varsigma^2(u,v)dv}du\\&=\frac{1}{Kn_{UT}}\frac{\int_0^{n_{BS}}\int_0^{Kn_{UT}}\varsigma^2(u,v)dudv}{n_{BS}-w\int_0^{n_{BS}}\int_0^{Kn_{UT}}\varsigma^2(u,v)dudv}\\&=q(\mathbf{\Sigma_M})\frac{1}{1-\frac{Kn_{UT}}{n_{BS}}wq(\mathbf{\Sigma_M})}\\&=\mathcal{R}_{q(\mathbf{\Sigma_M})\frac{1}{N}\mathbf{G_M}^\dagger\mathbf{G_M}}(w).\end{aligned} \tag{30}$$

where

$$q(\mathbf{\Sigma}_M)\triangleq\left\|\mathbf{\Sigma}_M\right\|^2/\left(KN^2n_{UT}n_{BS}\right) \tag{31}$$

is the Frobenius norm of the $\mathbf{\Sigma_M}$ matrix $\|\mathbf{\Sigma_M}\|\triangleq\sqrt{tr\left\{\mathbf{\Sigma_M}^\dagger\mathbf{\Sigma_M}\right\}}$ normalized with the matrix dimensions and

$$\begin{aligned}\left\|\mathbf{\Sigma}_M\right\|^2&=\mathrm{tr}\left\{\mathbf{\Sigma}_M^\dagger\mathbf{\Sigma}_M\right\}=\mathrm{tr}\left\{(\mathbf{\Sigma}\otimes\mathbf{J})^\dagger(\mathbf{\Sigma}\otimes\mathbf{J})\right\}\\&=\mathrm{tr}\left\{\left(\mathbf{\Sigma}^\dagger\otimes\mathbf{J}^\dagger\right)(\mathbf{\Sigma}\otimes\mathbf{J})\right\}=\mathrm{tr}\left\{\mathbf{\Sigma}^\dagger\mathbf{\Sigma}\otimes\mathbf{J}^\dagger\mathbf{J}\right\}\\&=\mathrm{tr}\left\{\mathbf{\Sigma}^\dagger\mathbf{\Sigma}\right\}\mathrm{tr}\left\{\mathbf{J}^\dagger\mathbf{J}\right\}=\mathrm{tr}\left\{\mathbf{\Sigma}^\dagger\mathbf{\Sigma}\right\}n_{UT}n_{BS}\\&=\left\|\mathbf{\Sigma}\right\|^2n_{UT}n_{BS}.\end{aligned} \tag{32}$$

Using Equations (31) and (32), it can be seen that

$$q(\mathbf{\Sigma}_M)=q(\mathbf{\Sigma})=\left\|\mathbf{\Sigma}\right\|^2/\left(KN^2\right) \tag{33}$$

In the asymptotic case, $q(\mathbf{\Sigma})$ is given by

$$\lim_{N\to\infty}q(\mathbf{\Sigma})=\frac{1}{K}\int_0^K\varsigma^2(u,v)dv. \tag{34}$$

The probability density function (p.d.f.) of the limiting eigenvalue distribution of $\frac{1}{N}\mathbf{H}^\dagger\mathbf{H}$ follows a scaled version of the Marčenko-Pastur law and hence the Shannon transform of the limiting eigenvalue distribution of $\frac{1}{N}\mathbf{H}^\dagger\mathbf{H}$ can be approximated by

$$\mathcal{V}_{\frac{1}{N}\mathbf{H}^\dagger\mathbf{H}}\left(\frac{\tilde{\gamma}}{Kn_{UT}}\right)\simeq\mathcal{V}_{\mathrm{MP}}\left(q(\mathbf{\Sigma})\frac{\tilde{\gamma}}{Kn_{UT}},\frac{Kn_{UT}}{n_{BS}}\right). \tag{35}$$

3) UT-side Correlated Cellular Channel : Assuming that there is no receive correlation at the BS side i.e $\mathbf{R_R}=\mathbf{I}$, the channel matrix of Equation (17) can be rewritten as follows:

$$\begin{aligned}\frac{1}{\sqrt{N}}\mathbf{H}&=\left(\mathbf{W}\left(\mathbf{I}_{KN}\otimes\mathbf{R_T}^{\frac{1}{2}}\right)\right)\\&\asymp\left(\mathbf{W}\left(\mathbf{I}_{KN}\otimes\mathbf{D_T}^{\frac{1}{2}}\right)\right)\end{aligned} \tag{36}$$

where $\mathbf{W} = \frac{1}{\sqrt{N}}\mathbf{\Sigma_M} \odot \mathbf{G_M}$ and therefore

$$\begin{aligned}\frac{1}{N}\mathbf{H}^{\dagger}\mathbf{H} &= \sum_{i=1}^{Nn_{BS}} \mathbf{h}_i^{\dagger}\mathbf{h}_i \\ &\asymp \sum_{i=1}^{Nn_{BS}} \left(\mathbf{I}_{KN} \otimes \mathbf{D_T}^{\frac{1}{2}}\right) \mathbf{w}_i^{\dagger}\mathbf{w}_i \left(\mathbf{I}_{KN} \otimes \mathbf{D_T}^{\frac{1}{2}}\right) \\ &= \sum_{i=1}^{Nn_{BS}} \left(\left(\mathbf{1}_{KN} \otimes \lambda_{\mathbf{T}}^{\frac{1}{2}}\right) \odot \mathbf{w}_i\right)^{\dagger} \left(\left(\mathbf{1}_{KN} \otimes \lambda_{\mathbf{T}}^{\frac{1}{2}}\right) \odot \mathbf{w}_i\right) \end{aligned} \tag{37}$$

where $\mathbf{w}_i$ denotes the ith $1 \times KNn_{UT}$ row vector of $\mathbf{W}$, $\mathbf{1}_{KN}$ is a $1 \times KN$ row vector of ones and $\lambda_{\mathbf{T}}$ is a row vector containing the eigenvalues of $\mathbf{R_T}$. Hence, the R-transform can be written as

$$\begin{aligned}\lim_{N\to\infty} R_{\frac{1}{N}\mathbf{H}^{\dagger}\mathbf{H}}(w) &= \lim_{N\to\infty} \sum_{i=1}^{Nn_{BS}} R_{\mathbf{h_i}^{\dagger}\mathbf{h_i}}(w) \\ &= \lim_{N\to\infty} \frac{1}{Kn_{UT}N} \sum_{i=1}^{Nn_{BS}} \frac{\|\mathbf{h}_i\|^2}{1 - w\|\mathbf{h}_i\|^2} \\ &= \frac{q(\Omega)}{1 - \frac{Kn_{UT}}{n_{BS}} w q(\Omega)} = \mathcal{R}_{q(\Omega)\frac{1}{N}\mathbf{G_M}^{\dagger}\mathbf{G_M}}(\omega) \end{aligned} \tag{38}$$

where

$$q(\mathbf{\Omega}) = \frac{\|\mathbf{h}_i\|^2}{KNn_{UT}} = \frac{\left\|\left(\mathbf{1}_{KN} \otimes \lambda_{\mathbf{T}}^{\frac{1}{2}}\right)\mathbf{w}_i\right\|^2}{KNn_{UT}} = \frac{1}{n_{UT}} \sum_{j=1}^{n_{UT}} \lambda_{\mathbf{T}}(j) \cdot \frac{1}{K} \int_0^K \varsigma^2\Big(u, v\Big) dv = \frac{1}{K} \int_0^K \varsigma^2\Big(u, v\Big) dv \tag{39}$$

It can be seen that the scaling of the Marčenko-Pastur law is identical for the cases of uncorrelated and UT-side correlated antennas, i.e. $q(\mathbf{\Sigma}) = q(\mathbf{\Omega})$. As a result, the per-cell capacity for UT-side correlation is given by (49) which coincides with the case of uncorrelated multiple antennas. Therefore, we can conclude for large values of K ($K \gg n_{UT}$) UT-side correlation has no effect on the system's performance. This ascertainment is expected, since the capacity scaling is dictated by the rank of the channel matrix $\mathbf{H}$, which depends only on the number of BS antennas in a cellular scenario.

4) BS-side Correlated Cellular Channel: Assuming that there is no transmit correlation at the UT side i.e. $\mathbf{R_T} = \mathbf{I}$, the channel matrix of Equation (17) can be rewritten as follows:

$$\begin{aligned}\frac{1}{\sqrt{N}}\mathbf{H} &= \left(\left(\mathbf{I}_N \otimes \mathbf{R_R}^{\frac{1}{2}}\right)\mathbf{W}\right) \\ &\asymp \left(\left(\mathbf{I}_N \otimes \mathbf{D_R}^{\frac{1}{2}}\right)\mathbf{W}\right) \end{aligned} \tag{40}$$

and therefore

$$\frac{1}{N}\mathbf{H}^{\dagger}\mathbf{H} = \frac{1}{N}\sum_{i=1}^{N}\mathbf{H}_i^{\dagger}\mathbf{H}_i = \sum_{i=1}^{N}\mathbf{W}_i^{\dagger}\mathbf{D_R}\mathbf{W}_i = \sum_{j=1}^{n_{BS}}\lambda_{\mathbf{R}}(j)\sum_{i=1}^{N}\mathbf{w}_i^{\dagger}\mathbf{w}_i \tag{41}$$

where $\mathbf{H}_i$ and $\mathbf{W}_i$ are submatrices of $\mathbf{H}$ and $\mathbf{W}$ respectively with dimensions $n_{BS} \times KNn_{UT}$ and $\lambda_{\mathbf{R}}$ is a row vector containing the eigenvalues of $\mathbf{R_R}$. Based on the previous analysis, the asymptotic eigenvalue distribution

of $\mathbf{A} = \sum_{i=1}^{N} \mathbf{w}_i^{\dagger}\mathbf{w}_i$ follows a scaled version of the Marčenko-Pastur law. Hence, the R-transform of $\mathbf{A}$ can be written as

$$\mathcal{R}_{\mathbf{A}}(w) \asymp \mathcal{R}_{q(\mathbf{\Sigma})\frac{1}{N}\tilde{\mathbf{G}}^{\dagger}\tilde{\mathbf{G}}}(w) = \frac{q(\mathbf{\Sigma})}{1 - Kn_{UT}wq(\mathbf{\Sigma})} \tag{42}$$

where $\tilde{\mathbf{G}}$ is a $N \times KNn_{UT}$ matrix distributed as $\mathcal{CN}(\mathbf{0}, \mathbf{I})$ and

$$q(\mathbf{\Sigma}) = \frac{\|\mathbf{w}_i\|^2}{KNn_{UT}} = \frac{1}{K}\int_0^K \varsigma^2\Big(u, v\Big)dv \tag{43}$$

The R-transform of $\frac{1}{N}\mathbf{H}^{\dagger}\mathbf{H}$ is calculated based on [18, Theorems 2.31 and 2.64]

$$\mathcal{R}_{\frac{1}{N}\mathbf{H}^{\dagger}\mathbf{H}}(w) = \sum_{j=1}^{n_{BS}} \lambda_{\mathbf{R}}(j)\mathcal{R}_{\mathbf{A}}(\lambda_{\mathbf{R}}(j)w). \tag{44}$$

The asymptotic eigenvalue pdf (AEPDF) of $\frac{1}{N}\mathbf{H}^{\dagger}\mathbf{H}$ is obtained by determining the imaginary part of the Cauchy transform $\mathcal{G}$ for real arguments

$$f^{\infty}_{\frac{1}{N}\mathbf{H}^{\dagger}\mathbf{H}}(x) = \lim_{y \to 0^+} \frac{1}{\pi}\Im\left\{\mathcal{G}_{\frac{1}{N}\mathbf{H}^{\dagger}\mathbf{H}}(x + jy)\right\} \tag{45}$$

considering that the Cauchy transform is derived from the R-transform [42] as follows

$$\mathcal{G}^{-1}_{\frac{1}{N}\mathbf{H}^{\dagger}\mathbf{H}}(w) = \mathcal{R}_{\frac{1}{N}\mathbf{H}^{\dagger}\mathbf{H}}(-w) - \frac{1}{w} \tag{46}$$

The AEPDF of $\frac{1}{N}\mathbf{H}\mathbf{H}^{\dagger}$ can be also derived as follows:

$$\frac{n_{BS}}{Kn_{UT}} f^{\infty}_{\frac{1}{N}\mathbf{H}^{\dagger}\mathbf{H}}(x) + (1 - \frac{n_{BS}}{Kn_{UT}})\delta(x) = f^{\infty}_{\frac{1}{N}\mathbf{H}^{\dagger}\mathbf{H}}(x) \tag{47}$$

since the matrices $\frac{1}{N}\mathbf{H}\mathbf{H}^{\dagger}$ and $\frac{1}{N}\mathbf{H}^{\dagger}\mathbf{H}$ have the same non zero eigenvalues, but their sizes differ by a factor of n_{BS}/Kn_{UT}.

5) Double-side Correlated Cellular Channel: By combining the two previous cases, it can be easily seen that the a.e.d. for the double-side Kronecker correlation model coincides with the BS-side correlation case, since UT-side correlation has no effect on the asymptotic eigenvalue distribution of $\frac{1}{N}\mathbf{H}^{\dagger}\mathbf{H}$. Figure 2 illustrates the AEPDF of $\frac{1}{N}\mathbf{H}^{\dagger}\mathbf{H}$ varying the level of correlation at the BS antennas ρ_R. As it can be seen, by increasing the level of fading correlation, the plot of the eigenvalue distribution is gradually decomposing into two segments.

C. Optimal Capacity

According to [18], the per-cell asymptotic Optimal Joint Decoding sum-rate capacity C_{opt} assuming a very large number of cells and no CSI available at the UT-side (e.g. uniform power allocation), is given by:

$$\begin{aligned} C_{\text{opt}}(\gamma, N, n_{BS}, K, n_{UT}) &= \lim_{N\to\infty} \frac{1}{N}\mathcal{I}\left(\mathbf{x};\mathbf{y} \mid \mathbf{H}\right) \\ &= \lim_{N\to\infty} \frac{1}{N}\mathbb{E}\left[\log\det\left(\mathbf{I} + \frac{\gamma}{n_{UT}}\mathbf{H}\mathbf{H}^{\dagger}\right)\right] \\ &= \lim_{N\to\infty} \mathbb{E}\left[\frac{1}{N}\sum_{i=1}^{Nn_{BS}} \log\left(1 + \frac{\tilde{\gamma}}{Kn_{UT}}\lambda_i\left(\frac{1}{N}\mathbf{H}\mathbf{H}^{\dagger}\right)\right)\right] \\ &= n_{BS}\int_0^{\infty} \log\left(1 + \frac{\tilde{\gamma}}{Kn_{UT}}x\right) f^{\infty}_{\frac{1}{N}\mathbf{H}\mathbf{H}^{\dagger}}(x)dx \\ &= Kn_{UT}\int_0^{\infty} \log\left(1 + \frac{\tilde{\gamma}}{Kn_{UT}}x\right) f^{\infty}_{\frac{1}{N}\mathbf{H}^{\dagger}\mathbf{H}}(x)dx \end{aligned} \tag{48}$$

where $\tilde{\gamma} = KN\gamma$ is the system transmit power normalized by the receiver noise power respectively and $\lambda_i\left(\mathbf{X}\right)$ denotes the eigenvalues of matrix $\mathbf{X}$. Equation (48) can be utilized in combination with Equation (45) and (46) for the case of correlated BS antennas. For uncorrelated BS antennas, the optimal per-cell sum-rate capacity is given by:

$$\begin{aligned} C_{\text{opt}}(\gamma, N, n_{BS}, K, n_{UT}) &= n_{BS}\mathcal{V}_{\frac{1}{N}\mathbf{H}\mathbf{H}^{\dagger}}\left(\tilde{\gamma}/Kn_{UT}\right) \\ &= n_{BS}Kn_{UT}\mathcal{V}_{\frac{1}{N}\mathbf{H}^{\dagger}\mathbf{H}}\left(\tilde{\gamma}/Kn_{UT}\right) \\ &\simeq n_{BS}Kn_{UT}\mathcal{V}_{\text{MP}}\left(q\left(\mathbf{\Sigma}\right)\frac{\tilde{\gamma}}{Kn_{UT}}, \frac{Kn_{UT}}{n_{BS}}\right). \end{aligned} \tag{49}$$

where $\mathcal{V}_{\text{MP}}$ is calculated based on Equation (21). It should be noted that if CSI is available at the UT-side, multiuser iterative waterfilling [43] can be employed to optimize the transmitter input and thus the produced capacity.

D. MMSE Capacity

A global joint decoder will be extremely demanding in terms of computational load as the complexity of symbol-by-symbol multiuser detection increases exponentially as the number of users to be detected in the system increases [36]. However, for a coded system MMSE in combination with Successive Interference Cancellation(SIC) yields linear complexity in the number of users, or at least polynomial if one considers that the computation of the MMSE filters, matrix-vector multiplications and subtraction are quadratic or cubic in the number of users [44, Chap. 8]. Based on this argument, the following equations describe the sub-optimal capacity achieved by a linear MMSE filter followed by single-stream decoding. Based on the arguments in [18, Equation 1.9][36], [45], [46], the MMSE and the Signal to Interference and Noise Ratio (SINR) for the kth date stream, assuming no CSI available at the UT-side (e.g. uniform power allocation), can be written as:

$$\begin{aligned} \text{mmse}_k &= \left[\left(\mathbf{I}_{KNn_{UT}} + \frac{\gamma}{n_{UT}}\mathbf{H}^{\dagger}\mathbf{H}\right)^{-1}\right]_{k,k}, \\ 1 + \text{SINR}_k &= 1 + \frac{1 - \text{mmse}_k}{\text{mmse}_k} = \text{mmse}_k^{-1}. \end{aligned} \tag{50}$$

Considering single-stream decoding, the per-cell asymptotic MMSE capacity is given by the mean individual stream rate multiplied by the number of streams per cell:

$$\begin{aligned}
C_{\mathrm{mmse}}(\gamma, N, n_{BS}, K, n_{UT}) &= \lim_{N\to\infty} Kn_{UT}\mathbb{E}\left[\log\left(\frac{1}{NKn_{UT}}\sum_{k=1}^{NKn_{UT}}(1+\mathrm{SINR}_k)\right)\right] \\
&\overset{(50)}{=} -\lim_{N\to\infty} Kn_{UT}\mathbb{E}\left[\log\left(\frac{1}{NKn_{UT}}\sum_{k=1}^{NKn_{UT}}\left[\left(\mathbf{I}_{NKn_{UT}}+\frac{\gamma}{n_{UT}}\mathbf{H}^{\dagger}\mathbf{H}\right)^{-1}\right]_{k,k}\right)\right] \\
&\leq -\lim_{N\to\infty} Kn_{UT}\log\left(\frac{1}{NKn_{UT}}\mathbb{E}\left[\mathrm{Tr}\left\{\left(\mathbf{I}_{NKn_{UT}}+\frac{\gamma}{n_{UT}}\mathbf{H}^{\dagger}\mathbf{H}\right)^{-1}\right\}\right]\right) \\
&= -\lim_{N\to\infty} Kn_{UT}\log\left(\mathbb{E}\left[\frac{1}{NKn_{UT}}\sum_{j=1}^{KNn_{UT}}\frac{1}{1+\frac{\tilde{\gamma}}{Kn_{UT}}\lambda_j\left(\frac{1}{N}\mathbf{H}^{\dagger}\mathbf{H}\right)}\right]\right) \\
&= -Kn_{UT}\log\left(\int_0^{\infty}\frac{1}{1+\frac{\tilde{\gamma}}{Kn_{UT}}x}f^{\infty}_{\frac{1}{N}\mathbf{H}^{\dagger}\mathbf{H}}(x)dx\right) \\
&= -Kn_{UT}\log\left(\int_{0^+}^{\infty}\frac{1}{1+\frac{\tilde{\gamma}}{Kn_{UT}}x}f^{\infty}_{\frac{1}{N}\mathbf{H}^{\dagger}\mathbf{H}}(x)dx + 1 - \frac{n_{BS}}{Kn_{UT}}\right) \qquad (51)
\end{aligned}$$

which can be utilized in combination with Equation (45) and (46) for the case of correlated BS antennas. For uncorrelated BS antennas, the asymptotic MMSE capacity is given by:

$$\begin{aligned}
C_{\mathrm{mmse}}(\gamma, N, n_{BS}, K, n_{UT}) &= -Kn_{UT}\log\left(\eta_{\frac{1}{N}\mathbf{H}^{\dagger}\mathbf{H}}\left(\frac{\tilde{\gamma}}{Kn_{UT}}\right)\right) \\
&= -Kn_{UT}\log\left(\eta_{\mathrm{MP}}\left(q\left(\mathbf{\Sigma}\right)\frac{\tilde{\gamma}}{Kn_{UT}}, \frac{Kn_{UT}}{n_{BS}}\right)\right), \qquad (52)
\end{aligned}$$

where η_{MP} is calculated based on Equation (22). In this point, it should be noted that MMSE filtering exhibits an interference-limited behavior, when the number of transmitters is larger than the number of receive antennas [4]. More specifically, in the previous transmission strategies the signals of all system UTs have been superpositioned on the shared time-frequency medium, which is sensible if optimal decoding is in place. However, if MMSE filtering is applied, the performance can be enhanced by orthogonalizing the intra-cell UTs so that only a single UT per cell transmits using the shared medium. This scenario resembles to cellular systems employing intra-cell TDMA, FDMA or orthogonal CDMA and its performance is evaluated in section V-A by means of Monte Carlo simulations.

V. Numerical Results

The analytical results (Equations (48),(49),(51),(52)) have been verified by running Monte Carlo simulations over 100 random instances of the system and by averaging the produced capacity results. More specifically, for each system instance the complex matrix $(\mathbf{I}_N \otimes \mathbf{R}_{\mathbf{R}}^{\frac{1}{2}})\mathbf{G}_{\mathbf{M}}$ is constructed by randomly generating correlated fading coefficients according to the exponential model with ρ_R being the BS-side correlation coefficient. UT-side correlation is not considered in the numerical results, since it does not have an effect on capacity for large K. Subsequently, the variance profile matrix $\mathbf{\Sigma}$ is constructed by randomly placing the UTs according to a uniform distribution in the planar coverage area and by calculating the variance profile coefficients using Equation (11). It should be noted

that the simulated system includes $N = 7$ BSs, which is adequately large to converge with the asymptotic analysis results. In the context of the mathematical analysis, the distance d_k^{nm} can be calculated assuming that the UTs are positioned on a uniform planar grid as in Fig. 1 [47]. The numerical results presented in this section refer to the optimal and MMSE per-cell sum-rate capacity averaged over a large number of fading realizations and UT positions. After constructing the channel matrix $\mathbf{H}$, the optimal per-cell sum-rate capacity is calculated by evaluating the formula in [20]

$$C_{\text{opt}} = \frac{1}{N}\mathbb{E}\left[\text{logdet}\left(\mathbf{I}_{Nn_{BS}} + \frac{\gamma}{n_{UT}}\mathbf{H}\mathbf{H}^{\dagger}\right)\right], \tag{53}$$

while the MMSE per-cell capacity is calculated by summing all the individual stream rates and normalizing by the number of cells [18]

$$C_{\text{mmse}} = -\frac{1}{N}\mathbb{E}\left[\sum_{k=1}^{NKn_{UT}} \log\left[\left(\mathbf{I}_{KNn_{UT}} + \frac{\gamma}{n_{UT}}\mathbf{H}^{\dagger}\mathbf{H}\right)^{-1}\right]_{k,k}\right], \tag{54}$$

where $[\mathbf{X}]_{k,k}$ denotes the kth diagonal element of the $\mathbf{X}$ matrix. In this context, Figures 3 and 4 depict the optimal and MMSE per-cell sum-rate capacity respectively versus the normalized cell radius R varying the level of receive correlation $\rho_R = [0, 0.9, 0.99, 1]$. As it can be observed in both cases, the BS-side correlation decreases the degrees of freedom due to the multiple receive antennas and therefore compromises the capacity performance of the system. In the no-correlation extreme $\rho_R = 0$, the optimal capacity curve is identical to the curve derived in [3] for multicell processing cellular systems with multiple antennas. In the full-correlation extreme $\rho_R = 1$, the capacity curve degrades to the single-antenna capacity [2], since no multiplexing gain is achieved by the multiple BS antennas. In the MMSE-receiver case, it can be seen that the achieved capacity in much lower than the optimal due to the lack of interference-suppressing dimensions, but the effect of correlation is less grave especially for short cell radii. It should be noted that in Figures 3 and 4 the analysis curve and the simulation points are marked using a solid line and circle points respectively in order to verify their close agreement. Subsequently, Figure 5 illustrates the per-cell sum-rate capacity versus the level of BS-side correlation for a fixed cell size. It can be observed that the optimal capacity degradation becomes detrimental for high correlation levels, whereas the MMSE receiver appears to be much more resistant to fading correlation. Finally, Figure 6 depicts the per-cell sum-rate capacity versus the normalized cell radius R varying the number of BS antennas n_{BS} for two values of correlation $\rho_R = [0, 0.8]$. By observing the figure, it becomes clear that the linear capacity scaling with the number of receive antennas n_{BS} remains in spite of the degrading effect of fading correlation.

A. Practical Results

This section aims at denormalizing the cellular system parameters employed in the analysis in order to present more practical numerical results. These results can be used to evaluate the capacity enhancement which BS cooperation can provide in the context of real-world cellular infrastructure. In this direction, if L_0 is the power loss at the reference distance d_0, the scaled variance profile function is given by

$$\varsigma(d(t)) = \sqrt{L_0\left(1 + \hat{d}(t)/d_0\right)^{-\eta}}. \tag{55}$$

The values of L_0 and η have been fitted to the path loss model defined in the "Urban Macro" scenario of [48]. Furthermore, the BS correlation level was selected according to [48] assuming 2 degrees angle spread, 50 degrees angle of arrival and an antenna spacing of 4λ, where λ is the communication wavelength. Table I includes a concise list of the nominal parameter values used for producing the results in Figure 7.

In addition, this section evaluates the performance of MMSE filtering in combination with intra-cell UT orthogonalization, so that it can be compared with the aforestudied wideband transmission cases. In this direction, a UT is randomly selected for each cell and their channel vectors are concatenated in order to construct the square $Nn_{UT} \times Nn_{UT}$ matrix $\mathbf{H}_{\text{orth}}$. Subsequently, the per-cell MMSE capacity is evaluated in accordance to equation (54):

$$C_{\text{mmse}}^{\text{orth}} = -\frac{1}{N}\mathbb{E}\left[\sum_{k=1}^{Nn_{UT}} \log\left[\left(\mathbf{I}_{Nn_{UT}} + \frac{\gamma}{n_{UT}}\mathbf{H}_{\text{orth}}^{\dagger}\mathbf{H}_{\text{orth}}\right)^{-1}\right]_{k,k}\right]. \tag{56}$$

It is interesting that in the considered parameter range, the effect of both BS-side correlation and cell density on the MMSE capacity is negligible due to the interference-limited behavior which has also been observed in [4], [29]. On the contrary, the optimal capacity performance is degraded by 1 bit/sec/Hz due to correlation, which is acceptable considering the high spectral efficiency enhancement due to multicell processing. Furthermore, it can be observed that for $n_{BS} \geq n_{UT}$ the performance of MMSE filtering combined with intra-cell orthogonalization is no longer interference-limited, since there are sufficient degrees of freedom to suppress inter-cell interference.

VI. Conclusion

In this paper, we have considered a multicell processing system with MIMO links and distributed UTs. In this context, we have investigated the effect of antenna correlation on the capacity performance of the system. The presented results has been derived considering that the variances of the Gaussian channel gains are scaled by a generic variance profile which incorporates both path loss and antenna correlation. In this direction, we have presented two analytical approaches: a finite Random Matrix Theory approach and an asymptotic Free Probability approach. The former approach is useful for reducing the complexity of capacity calculation in finite systems, whereas the latter provides closed forms and interesting insights on the system performance. The main findings can be summarized as follows: antenna correlation degrades the capacity performance of the system, especially if it appears on the BS side. What is more, for large number of UTs per cell, the effect of UT-side correlation is negligible. Finally, it is shown that the MMSE performance is greatly suboptimal but more resilient to fading correlation in comparison to optimal decoding.

Acknowledgment

The work reported in this paper has formed part of the "Fundamental Limits to Wireless Network Capacity" Elective Research Programme of the Virtual Centre of Excellence in Mobile & Personal Communications, Mobile VCE, www.mobilevce.com. This research has been funded by the following Industrial Companies who are Members of Mobile VCE - BBC, BT, Huawei, Nokia, Nokia Siemens Networks, Nortel, Vodafone. Fully detailed technical

reports on this research are available to staff from these Industrial Members of Mobile VCE. The authors would like to thank Prof. G. Caire and Prof. D. Tse for the useful discussions.

REFERENCES

[1] O. Somekh and S. Shamai, "Shannon-theoretic approach to a Gaussian cellular multiple-access channel with fading," *IEEE Trans. Inform. Theory*, vol. 46, no. 4, pp. 1401–1425, Jul 2000.

[2] S. Chatzinotas, M. Imran, and C. Tzaras, "On the capacity of variable density cellular systems under multicell decoding," *IEEE Commun. Lett.*, vol. 12, no. 7, pp. 496 – 498, Jul 2008.

[3] ——, "Uplink capacity of MIMO cellular systems with multicell processing."

[4] H. Dai and H. Poor, "Asymptotic spectral efficiency of multicell mimo systems with frequency-flat fading," *IEEE Trans. Signal Processing*, vol. 51, no. 11, pp. 2976–2988, Nov 2003.

[5] D. Aktas, M. Bacha, J. Evans, and S. Hanly, "Scaling results on the sum capacity of cellular networks with mimo links," *IEEE Trans. Inform. Theory*, vol. 52, no. 7, pp. 3264–3274, July 2006.

[6] D.-S. Shiu, G. Foschini, and M. G. J. Kahn, "Fading correlation and its effect on the capacity of multielement antenna systems," *Communications, IEEE Transactions on*, vol. 48, no. 3, pp. 502–513, Mar 2000.

[7] C.-N. Chuah, D. Tse, J. Kahn, and R. Valenzuela, "Capacity scaling in MIMO wireless systems under correlated fading," *IEEE Trans. Inform. Theory*, vol. 48, no. 3, pp. 637–650, Mar 2002.

[8] W. Hachem, O. Khorunzhiy, P. Loubaton, J. Najim, and L. Pastur, "A new approach for capacity analysis of large dimensional multi-antenna channels," 2006, submitted to IEEE Transactions on Information Theory.

[9] D. Gesbert, H. Bolcskei, D. Gore, and A. Paulraj, "Outdoor MIMO wireless channels: models and performance prediction," *Communications, IEEE Transactions on*, vol. 50, no. 12, pp. 1926–1934, Dec 2002.

[10] J. Kermoal, L. Schumacher, K. Pedersen, P. Mogensen, and F. Frederiksen, "A stochastic MIMO radio channel model with experimental validation," *IEEE J. Select. Areas Commun.*, vol. 20, no. 6, pp. 1211–1226, Aug 2002.

[11] D. Chizhik, G. Foschini, and R. Valenzuela, "Capacities of multi-element transmit and receive antennas: Correlations and keyholes," *Electronics Letters*, vol. 36, no. 13, pp. 1099–1100, 2000.

[12] D. Chizhik, G. Foschini, M. Gans, and R. Valenzuela, "Keyholes, correlations, and capacities of multielement transmit and receive antennas," *IEEE Trans. Wireless Commun.*, vol. 1, no. 2, pp. 361–368, Apr 2002.

[13] C. Martin and B. Ottersten, "Asymptotic eigenvalue distributions and capacity for MIMO channels under correlated fading," *IEEE Trans. Wireless Commun.*, vol. 3, no. 4, pp. 1350–1359, Jul 2004.

[14] X. Mestre, J. Fonollosa, and A. Pages-Zamora, "Capacity of MIMO channels: asymptotic evaluation under correlated fading," *IEEE J. Select. Areas Commun.*, vol. 21, no. 5, pp. 829–838, June 2003.

[15] A. Skupch, D. Seethaler, and F. Hlawatsch, "Free probability based capacity calculation for MIMO channels with transmit or receive correlation," *Wireless Networks, Communications and Mobile Computing, 2005 International Conference on*, vol. 2, pp. 1041–1046 vol.2, 13-16 June 2005.

[16] S. Loyka, "Channel capacity of MIMO architecture using the exponential correlation matrix," *Communications Letters, IEEE*, vol. 5, no. 9, pp. 369–371, Sep 2001.

[17] H. Shin, M. Win, and M. Chiani, "Asymptotic statistics of mutual information for doubly correlated MIMO channels," *IEEE Trans. Wireless Commun.*, vol. 7, no. 2, pp. 562–573, Feb 2008.

[18] A. M. Tulino and S. Verdu, "Random matrix theory and wireless communications," *Commun. Inf. Theory*, vol. 1, no. 1, pp. 1–182, 2004.

[19] R. Muller, "A random matrix model of communication via antenna arrays," *IEEE Trans. Inform. Theory*, vol. 48, no. 9, pp. 2495–2506, Sep 2002.

[20] I. E. Telatar, "Capacity of multi-antenna Gaussian channels," *European Transactions on Telecommunications*, vol. 10, no. 6, pp. 585–595, Nov 1999.

[21] G. J. Foschini and M. J. Gans, "On limits of wireless communications in a fading environment when using multiple antennas," *Wirel. Pers. Commun.*, vol. 6, no. 3, pp. 311–335, 1998.

[22] A. Tulino, A. Lozano, and S. Verdu, "Impact of antenna correlation on the capacity of multiantenna channels," *IEEE Trans. Inform. Theory*, vol. 51, no. 7, pp. 2491–2509, Jul 2005.

[23] A. Sengupta and P. Mitra, “Capacity of multivariate channels with multiplicative noise: Random matrix techniques and large-n expansions (2),” *Journal of Statistical Physics*, vol. 125, pp. 1223–1242(20), December 2006.

[24] E. Jorswieck and H. Boche, “Performance analysis of MIMO systems in spatially correlated fading using matrix-monotone functions,” *IEICE Transactions*, vol. 89-A, no. 5, pp. 1454–1472, 2006.

[25] ——, “Majorization and matrix-monotone functions in wireless communications,” *Found. Trends Commun. Inf. Theory*, vol. 3, no. 6, pp. 553–701, 2006.

[26] A. Moustakas and S. Simon, “On the outage capacity of correlated multiple-path MIMO channels,” *IEEE Trans. Inform. Theory*, vol. 53, no. 11, pp. 3887–3903, Nov. 2007.

[27] G. Taricco, “Asymptotic mutual information statistics of separately-correlated Rician fading MIMO channels,” 2007, submitted to the IEEE Transactions on Information Theory. [Online]. Available: http://arxiv.org/abs/0712.4011

[28] A. Wyner, “Shannon-theoretic approach to a Gaussian cellular multiple-access channel,” *IEEE Trans. Inform. Theory*, vol. 40, no. 6, pp. 1713–1727, Nov 1994.

[29] N. Letzepis, “Gaussian cellular muptiple access channels,” Ph.D. dissertation, Institute for Telecommunications Research, University of South Australia, Dec 2005.

[30] S. Chatzinotas, M. Imran, and R. Hoshyar, “Multicell decoding sum-rate and user-rate shares of the cellular MIMO uplink channel,” 2009, submitted to IEEE Transactions on Communications.

[31] T. M. Cover and J. A. Thomas, *Elements of information theory*. New York, NY, USA: Wiley, 2005.

[32] L. Ong and M. Motani, “On the capacity of the single source multiple relay single destination mesh network,” *Ad Hoc Netw.*, vol. 5, no. 6, pp. 786–800, 2007.

[33] W. Hachem, P. Loubaton, and J. Najim, “Deterministic equivalents for certain functionals of large random matrices,” *Annals of Applied Probability*, vol. 17, pp. 875–930,, 2007. [Online]. Available: http://arxiv.org/abs/math.PR/0507172

[34] D. Voiculescu, “Asymptotically commuting finite rank unitary operators without commuting approximants,” *Acta Sci. Math.*, vol. 45, pp. 429–431, 1983.

[35] V. Marcenko and L. Pastur, “Distributions of eigenvalues of some sets of random matrices,” *Math. USSR-Sb.*, vol. 1, pp. 507–536, 1967.

[36] S. Verdu, *Multiuser Detection*. UK: Canbridge University Press, 1998.

[37] T. Ratnarajah and R. Vaillancourt, “Complex random matrices and applications,” *Computer & Mathematics with Applications*, vol. 50, no. 3-4, pp. 399–411, Aug 2005.

[38] R. Tempo, G. Calafiore, and F. Dabbene, *Randomized Algorithms for Analysis and Control of Uncertain Systems*, ser. Communications and Control Engineering Series. London: Springer, 2005.

[39] F. Hiai and D. Petz, “Asymptotic freeness almost everywhere for random matrices,” *Acta Sci. Math. (Szeged)*, vol. 66, pp. 801–826, 2000.

[40] M. Peacock, I. Collings, and M. Honig, “Asymptotic spectral efficiency of multiuser multisignature CDMA in frequency-selective channels,” *IEEE Trans. Inform. Theory*, vol. 52, no. 3, pp. 1113–1129, Mar 2006.

[41] W. Hachem, “Low complexity polynomial receivers for downlink CDMA,” *Signals, Systems and Computers, 2002. Conference Record of the Thirty-Sixth Asilomar Conference on*, vol. 2, pp. 1919–1923 vol.2, Nov 2002.

[42] N. Raj Rao and A. Edelman, “The polynomial method for random matrices,” *Foundations of Computational Mathematics*, 2007.

[43] W. Yu, W. Rhee, S. Boyd, and J. Cioffi, “Iterative water-filling for Gaussian vector multiple-access channels,” *IEEE Trans. Inform. Theory*, vol. 50, no. 1, pp. 145–152, Jan. 2004.

[44] D. Tse and P. Viswanath, *Fundamentals of Wireless Communications*. University Press, Cambridge, 2005.

[45] U. Madhow and M. Honig, “Mmse interference suppression for direct-sequence spread-spectrum cdma,” *IEEE Trans. Commun.*, vol. 42, no. 12, pp. 3178–3188, Dec 1994.

[46] D. Tse and S. Hanly, “Linear multiuser receivers: effective interference, effective bandwidth and user capacity,” *IEEE Trans. Inform. Theory*, vol. 45, no. 2, pp. 641–657, Mar 1999.

[47] S. Chatzinotas, M. Imran, and C. Tzaras, “Optimal information theoretic capacity of planar cellular uplink channel,” in *Signal Processing Advances in Wireless Communications, 9th IEEE International Workshop on (SPAWC’08)*, Recife, Pernambuco, Brazil, Jul 2008, pp. 196 – 200.

[48] ETSI TR 125 996 V7.0.0, “Universal mobile telecommunications system (UMTS); spatial channel model for multiple input multiple output (MIMO) simulations (3GPP TR 25.996 ver. 7.0.0 rel. 7),” Jun 2007.

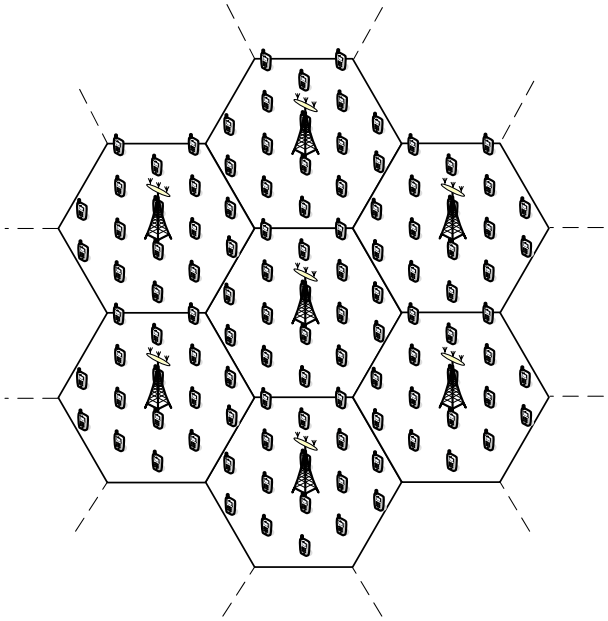

Fig. 1. Ground plan of the cellular system comprising of BSs with multiple antennas and UTs distributed on a uniform hexagonal grid.

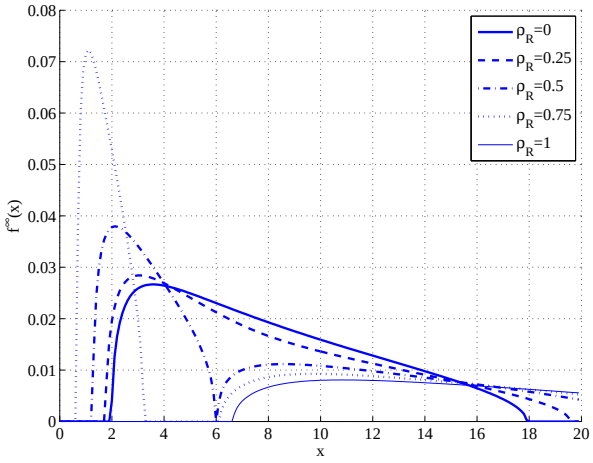

Fig. 2. Asymptotic Eigenvalue Probability Distribution Function (AEPDF) of $\frac{1}{N}\mathbf{H}^{\dagger}\mathbf{H}$ (omitting the zero eigenvalues) while varying the level of correlation at the BS antennas ρ_R. Parameters: $K = 4, n_{UT} = 2, n_{BS} = 2, \eta = 2, \gamma = 10$.

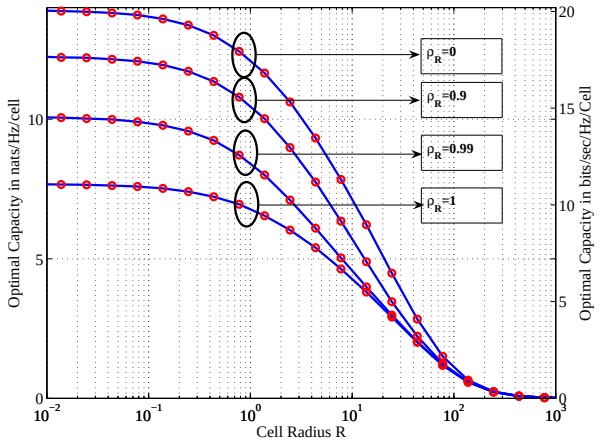

Fig. 3. Optimal per-cell sum-rate capacity vs. the normalized cell Radius R varying the level of BS-side correlation $\rho_R = [0, 0.9, 0.99, 1]$ in a planar cellular system with uniformly distributed UTs. Analysis curve and simulation points are marked using a solid line and circle points respectively. Parameters: $K = 16, \gamma = 10, n_{BS} = 2, n_{UT} = 1, \eta = 2$.

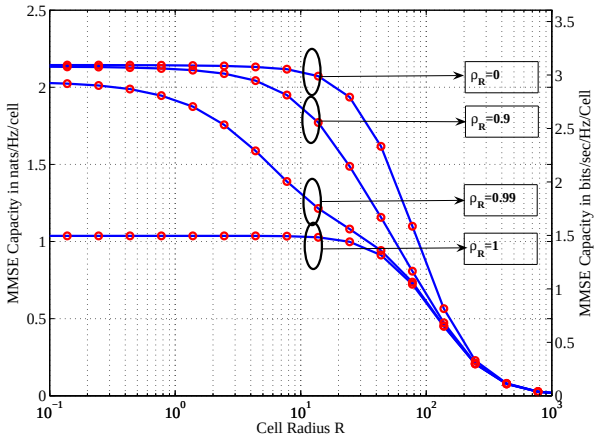

Fig. 4. MMSE per-cell sum-rate capacity vs. the normalized cell Radius R varying the level of BS-side correlation $\rho_R = [0, 0.9, 0.99, 1]$ in a planar cellular system with uniformly distributed UTs. Analysis curve and simulation points are marked using a solid line and circle points respectively. Parameters: $K = 16, \gamma = 10, n_{BS} = 2, n_{UT} = 1, \eta = 2$.

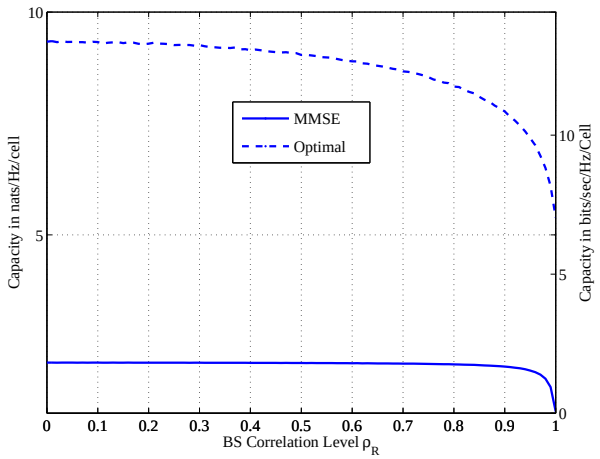

Fig. 5. Optimal and MMSE per-cell sum-rate capacity vs. the level of BS-side correlation ρ_R for a fixed-radius cellular system with uniformly distributed UTs. Parameters: $K = 16, \gamma = 10, n_{BS} = 2, n_{UT} = 1, \eta = 2$.

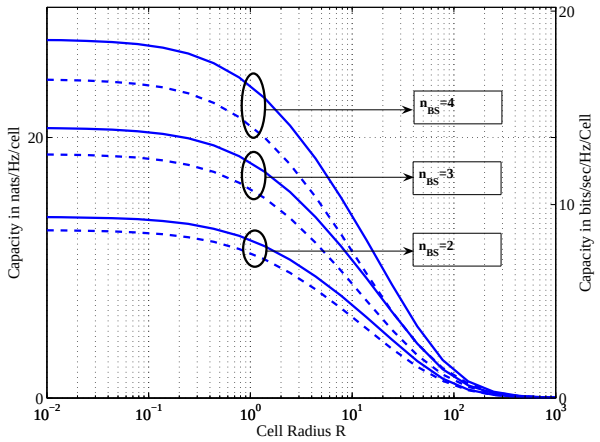

Fig. 6. Optimal per-cell sum-rate capacity vs. the normalized cell Radius R varying the number of BS antennas n_{BS} for two values of receive correlation $\rho_R = [0, 0.8]$ (solid and dashed line respectively) in a planar cellular system with uniformly distributed UTs. Parameters: $K = 16, \gamma = 10, n_{UT} = 1, \eta = 2$.

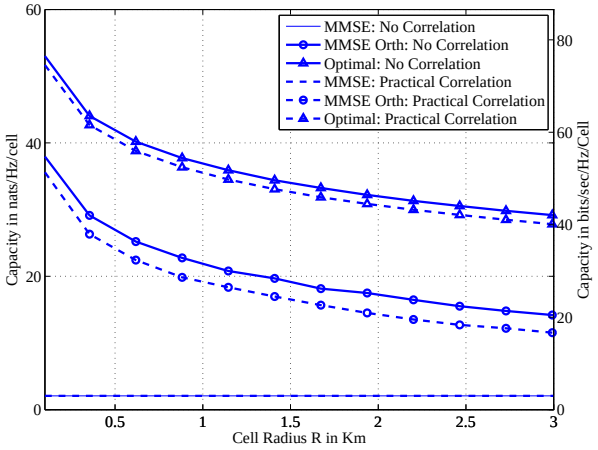

Fig. 7. Optimal and MMSE per-cell sum-rate capacity vs. the cell Radius R in Km considering the practical parameters in Table I.

TABLE I

PARAMETERS FOR PRACTICAL CELLULAR SYSTEMS

Parameter	Symbol	Value/Range (units)
Cell Radius	R	$0.1 - 3\ Km$
Reference Distance	d_0	$1\ m$
Reference Path Loss	L_0	$34.5\ dB$
Path Loss Exponent	η	3.5
Antennas per BS	n_{BS}	2
BS Correlation Level	ρ_R	0.8624
Antennas per UT	n_{UT}	2
UTs per Cell	K	16
UT Transmit Power	P_T	$200\ mW$
Thermal Noise Density	N_0	$-169\ dBm/Hz$
Channel Bandwidth	B	$5\ MHz$